


Gradient sensing via cell communication

Dallas Foster *Department of Mathematics, Oregon State University, Corvallis, Oregon 97331, USA*Brian Frost-LaPlante *Department of Electrical Engineering, Columbia University, New York, New York 10027, USA*

Collin Victor

*Department of Mathematics, University of Nebraska at Lincoln, Lincoln, Nebraska 68588, USA*Juan M. Restrepo *Computer Science and Mathematics Division, Oak Ridge National Laboratory, Oak Ridge, Tennessee 37831, USA
and Kavli Institute for Theoretical Physics, University of California, Santa Barbara, Santa Barbara, California 93106, USA*

(Received 15 April 2020; revised 18 November 2020; accepted 25 January 2021; published 15 February 2021; corrected 22 March 2021)

Experimental evidence lends support to the conjecture that cell-to-cell communication plays a role in the gradient sensing of chemical species by certain chains of cells. Models have been formulated to explore this idea. For cells with no identifiable sensing structure, Mugler *et al.* [*Proc. Natl. Acad. Sci. (U.S.A.)* **113**, E689 (2016)] have defined a particular local excitation, global inhibition (LEGI) model that pits nearest-neighbor communication against local reactions in a noisy environment to suggest how this sensing capability might arise in a physical system. In this study, we generalize the nearest-neighbor communication mechanism in the aforementioned LEGI model in order to explore the extent to which the gradient sensing characteristics depend on the parametrization of the communication itself, as well as on the cell size, the radius of influence of neighboring cells, and the influence of the background noise. Using our generalization and a collection of particular candidate communication models, we find that the precision of gradient sensing is indeed sensitive to the particular communication model, and we derive physical and analytic explanations for these results. The framework established and the associated results should prove useful in understanding the appropriateness of particular cell-to-cell communication models in gradient sensing studies.

DOI: [10.1103/PhysRevE.103.022405](https://doi.org/10.1103/PhysRevE.103.022405)

I. INTRODUCTION

The motion and biased growth in organisms as a consequence of exposure to a chemical component gradient are two manifestations of what is called chemotaxis. Chemotaxis plays a role in wound healing, neuronal network development, and tumor metastasis. Determining how cells detect such a gradient, and the extent of this capability, are critical to understanding the individual and collective dynamics of cellular chemotaxis.

Studies aimed at understanding chemotactic gradient sensing have traditionally focused on the physical capabilities of a single cell [1–3]. It is now clear that limiting ourselves to understanding single-cell gradient sensing does not generally explain chemotaxis for certain collections of cells [4,5], particularly when the cells in question do not have any apparent dedicated organelle that can sense spatial chemical species biases [3,6–8].

Cell-to-cell communication is a signaling pathway, potentially critical in cell chemotaxis. Signaling is common among cell networks; however, one could imagine that an intercellular signal would have to compete with substantial background

noise, and thus it is not obvious whether communication could be a significant actor in gradient sensing. In fact, experiments have demonstrated that it is the norm, rather than the exception, for the concentration of ambient chemical species in the environment itself to be noisy (see Berg and Purcell [1], who first made this point in analyzing the sensing of a gradient by a single cell) and, as a possible consequence, interfere with the cell's ability to react to a bias in the exterior field of chemical species [9–12].

The local excitation global inhibition (LEGI) framework proposes that the dynamics of a receptor-chemical species reaction internal to a cell is influenced by both local and remote externalities [2,3]. The LEGI framework has been extended to incorporate interactions between cells that form part of a chain [7,13,14]. Mugler *et al.* [14], using an adaptation of the LEGI approach, proposed a model in which each cell of a chain has internal cell receptors that sense the local external chemical species field and the concentrations present in neighboring cells via distinct, separate receptors. The latter receptors are thus called communication receptors. In developing their model, they proposed the simplest possible communication scheme, namely by each cell that

interacted with its nearest neighbors. Their model includes a local reaction, coupled with an external diffusive chemical species and cell-to-cell communication. The background noise is parametrized by a stochastic process. Using physically inspired ranges for model parameters, they were able to determine that their modeled cells can discern differences in the internal and the communicated signals even when taking into account noise (see also [9]). This modeling outcome suggests that cells may be able to sense gradients via communication.

Obviously, exploring cell chain gradient sensing via models also depends critically on how the processes are captured in the model, and most critically, on how the communication mechanism itself is formulated. The nearest-neighbor communication scheme is the simplest formulation with a physically plausible mechanism, but are the induced properties more appropriate than other models? Work remains to be done on the experimental side to describe and understand the specifics of the communication mechanism relevant to gradient sensing. Given this uncertainty, we are motivated to examine several alternative communication models. This paper generalizes the model advanced by Mugler *et al.* [14] by introducing a broad framework for the parametrization of cell interaction. This opens the way for us to systematically analyze several communication models that result from various specializations of the general framework. In doing so, we can compare various models with regard to their impact on chemical species sensing in a noisy environment.

This study explores how adopting various alternative models for communication, derived from a common general framework, affects the modeled ability of cell collections to sense a gradient as measured by the signal-to-noise ratio (SNR). The SNR was suggested by Mugler *et al.* as a way to quantify gradient sensing. We will analyze this collection of models in order to assess how cell size and intercellular communication radius affect three model outcomes. First, we estimate the phase and group velocities in order to better understand how signals and disturbances evolve (spectrally) as they move through the chain, along the way enhancing or suppressing the ever present noise that accompanies these. Second, we compare how the various model alternatives affect concentration correlations. Finally, the various specializations of the general framework are compared with respect to their SNR, interpreted according to the preceding physical qualities.

II. THE NEAREST-NEIGHBOR LEGI MODEL

The evolutionary model due to Mugler *et al.* [14] captures the reaction equations of a one-dimensional chain of cells, exposed to a diffusing external chemical species. Its distinguishing feature is the presence of nearest-neighbor, cell-to-cell communication of an internal chemical species. We refer to this model as the nearest-neighbor LEGI (NNLEGI) model. We refer the reader to [14] for the full details. Our presentation is brief and is mainly used to introduce notation and our choice of scaling.

Consider a chain of m cells, each of length a , that are placed in a field of a diffusing chemical species $c(z, t)$, where z represents position and t is time. The dynamics of $c(z, t)$

TABLE I. Model parameters and their values (from [14]).

Name	Symbol	Value	Units of
No. of cells	m	6–100	(1)
Cell length	a	10×10^{-6}	(m)
Mean external concentration	c_0	$\approx 10^{-9}$	(mol)
Diffusion coefficient	D	50×10^{-6}	($\text{m}^2 \text{s}^{-1}$)
Receptor binding rate	α	10^5	(s^{-1})
Receptor unbinding rate	μ	1	(s^{-1})
Intercellular activation rate	β	100	(s^{-1})
Intercellular deactivation rate	ν	1	(s^{-1})
Intercellular communication rate	γ	100	(s^{-1})

are governed by the diffusion equation, with diffusion coefficient D . The n th cell in the chain, located at z_n , has an active receptor r_n that binds and unbinds the external field $c(z_n, t) := c_n$ with rate α and μ , respectively. The receptor also activates the local and communicable species $x_n(t)$ and $y_n(t)$ at the rate β . x is local to each cell while y can be shared among neighbor cells at a constant rate γ and in a manner modeled using a communication matrix denoted by M . The receptor, local, and communicable species are subject to thermal fluctuations. x and y are activated and deactivated at the same rate, but the exchange of y between cells leads to differences in the concentration of x and y in each cell. This difference between the local and global concentrations is proposed to be the underlying signal the cell uses to infer the gradient of the external chemical field. For a summary of these parameters and corresponding values, see Table I.

We nondimensionalize this system by dividing length scales z and a by the total length of the system L , multiplying t by D/L^2 , and multiplying the concentration of each species by $1/c_0$, where c_0 is a reference external concentration. Each rate α , β , μ , ν , and γ is similarly nondimensionalized by scaling by a factor of a^2/D . Nondimensionalized, the NNLEGI model is

$$\begin{aligned} \dot{c} &= \nabla^2 c - \sum_{n=1}^m \delta\left(\frac{z}{L} - \frac{z_n}{L}\right) \frac{dr_n}{dt}, \\ \dot{r}_n &= \alpha c_n - \mu r_n + \eta_n, \\ \dot{x}_n &= \beta r_n - \nu x_n + \xi_n, \\ \dot{y}_n &= \beta r_n - \nu \sum_{n'=1}^m M_{nn'} y_{n'} + \chi_n, \end{aligned} \quad (2.1)$$

where $\delta(z)$ is the (spatial) Dirac delta, dot notation refers to the temporal derivative, and $n = 1, \dots, m$. M is given explicitly by

$$M_{nn'} = \delta_{n,n'}(1 + 2\gamma/\nu) - (\delta_{n-1,n'} + \delta_{n+1,n'})\gamma/\nu,$$

where $\delta_{i,j}$ is the Kronecker delta. η_n , ξ_n , and χ_n are the noise terms. As argued in [14], $\eta_n = \alpha \bar{c}_n \delta F_n$ comes from the “equilibrium binding and unbinding of external molecules to receptors” and is in terms of δF_n , the free-energy difference associated with a molecule unbinding from the n th cell. The units of F_n are those of the Boltzmann constant times temperature. The zero-mean noise terms, representing thermal effects,

obey

$$\begin{aligned} \langle \xi_n(t) \xi_{n'}(t') \rangle &= \delta_{nn'} (\beta \bar{r}_n + \nu \bar{x}_n) \delta(t - t'), \\ \langle \chi_n(t) \chi_{n'}(t') \rangle &= [\delta_{nn'} (\beta \bar{r}_n + \nu \bar{y}_n + 2\gamma \bar{y}_n + \gamma \bar{y}_{n-1} + \gamma \bar{y}_{n+1}) \\ &\quad - \delta_{n-1, n'} (\gamma \bar{y}_{n-1} + \gamma \bar{y}_{n+1}) \\ &\quad - \delta_{n+1, n'} (\gamma \bar{y}_{n-1} + \gamma \bar{y}_{n+1})] \delta(t - t'), \end{aligned} \quad (2.2)$$

where $\delta(t)$ represents the temporal Dirac delta. Positive terms account for the Poisson noise and negative terms account for the anticorrelation from each exchange. \bar{c} , \bar{r} , \bar{x} , and \bar{y} represent mean steady-state solutions, which will be explicitly described in Sec. IV B.

III. GENERALIZATION OF THE NNLEGI MODEL

We consider a limiting generalization of Eq. (2.1) where the number of cells is very large, i.e., $m \rightarrow \infty$ and $a \rightarrow 0$. Heuristically, this represents the limit of indistinguishable cells as the cell size is negligible compared to the size of the domain overall. In this limit, the resulting set of partial differential equations can be written as

$$\begin{aligned} \dot{c} &= \nabla^2 c - \int_{\mathcal{C}} \delta(z - z^*) \dot{r} dz^*, \\ \dot{r} &= (\alpha c - \mu r) + \eta, \\ \dot{x} &= \beta r - \nu x + \xi, \\ \dot{y} &= \beta r - \nu y + \gamma (w * y) + \chi \end{aligned} \quad (3.1)$$

for $t > 0$ and $z \in \Omega$, the physical domain. $c(z, t)$, $r(z, t)$, $x(z, t)$, and $y(z, t)$ represent continuous concentrations and are assumed known at $t = 0$. The random processes $\eta(z, t)$, $\xi(z, t)$, and $\chi(z, t)$ are now functions of space and time. We will refer to the term $(w * y)$ as the *communication term*. It is the convolution of y and a weight function (kernel) $w(z)$. The (spatial) convolution is defined as

$$(w * y)(z, t) := \int_{-\infty}^{\infty} w(u) y(z - u, t) du. \quad (3.2)$$

Certain integrability properties need to be imposed on the kernel w for this general communication term to be well-defined. In the following section, we will show that the simplest approximation of the communication term in fact leads to the NNLEGI model; however, the manner in which this generalized communication term is approximated leads to several other alternative LEGI models with communication. The purpose of this exposition is to provide a flexible

framework of models that captures a wide range of qualitative model outcomes.

A. Alternative communication models

To investigate the impact of the communication model in Eq. (3.1), we focus on the convolution kernel w . The goal of this section is not only to derive candidate functions for w , but to provide a motivation for these candidates, and to understand how various candidates approximate the convolution term in Eq. (3.2), what errors are invoked during the approximation, and what physical properties can be expected when employing them. When the diffusion scale is small compared to the correlation length of communication, the manner in which the kernel is mapped onto a discrete cell chain becomes important. Specifically, some approximations lead to a sensitive dependence of gradient sensing estimates on the nature of the kernel. In the discussion that follows, we make use of finite-difference approximation notation and terminology; for reference, see [15] or similar text.

We make several simplifying assumptions about the physical properties of w . First, the kernel cannot have a net effect on the total amount of the global intercellular species. Hence, the kernel w has the zero-sum property

$$\int_{\mathcal{C}} w(z) dz = 0. \quad (3.3)$$

Secondly, in order to make comparisons with the outcomes in [14], we specifically limit our analysis to kernels w that do not endow directional preferences to the fluxes of concentration. In other words, we are assuming that w should be spatially symmetric, i.e., w is an even function about the origin, and, as a result, the integral of the product of $w(z)$ with an odd function about the domain \mathcal{C} will be zero. This last property will be important for deriving the generalized models.

An example of a continuous kernel that satisfies these properties, w^c , which we will use to compare the behavior of the approximations to, is

$$w^c(z) := \frac{d^2}{dz^2} \frac{ae^{-z^2/2a^2}}{\sqrt{2\pi}}. \quad (3.4)$$

We analyze the communication operator when the support of w is small by using a series expansion approach. As in [16], we expand y into a Taylor series centered at z , obtaining, to lowest order, a second-order operator approximation. To see this,

$$\begin{aligned} \int_{-\infty}^{\infty} w(u) y(z - u, t) du &\approx \int_{-\infty}^{\infty} w(u) \left(y(z, t) - uy'(z, t) + \frac{u^2}{2} y''(z, t) + O(u^3 y^{(3)}) \right) du \\ &\approx y(z, t) \int_{-\infty}^{\infty} w(u) du - y'(z, t) \int_{-\infty}^{\infty} w(u) u du + y''(z, t) \int_{-\infty}^{\infty} \frac{u^2}{2} w(u) du. \end{aligned} \quad (3.5)$$

The symmetry and zero-sum assumptions of w imply that the first two terms in the preceding integral expression are zero. The remaining term is a number solely dependent on the structure of the kernel in use. We call this number Γ_1 , allowing

us to simply write

$$w * y \approx y''(z, t) \int_{-\infty}^{\infty} \frac{u^2}{2} w(u) du = \Gamma_1 y''(z, t).$$

Substituting this approximation into Eq. (3.1), we obtain the differential equation,

$$\dot{y} = \beta r(z, t) - \nu y(z, t) + \Gamma_1 \gamma y''(z, t) + \xi. \quad (3.6)$$

That is, we find that when the convolution kernel w has relatively small support, i.e., communication can only be shared among a small fraction of the cells in the entire chain of cells in a given time, then the convolution can be approximated to second order with a second derivative operator. The accuracy of this approximation is in terms of, and depends on, the smoothness of y , since the magnitude of the terms being neglected is dominated by the behavior of higher derivatives of y and the support of the kernel w . To investigate the consequence of the order of approximation of the convolution, we will also consider the next highest order of convolution approximation, a fourth-order approximation (the third-order term drops out as a result of the symmetry assumption on w),

$$\dot{y} = \beta r(z, t) - \nu y(z, t) + \Gamma_1 \gamma y''(z, t) + \Gamma_2 \gamma y^{(4)}(z, t) + \chi, \quad (3.7)$$

where $\Gamma_2 = \int w(u)u^4/24 du$.

Up to this point, we have considered a continuous chain of cells. To compare our results with those of Mugler *et al.*, we must ultimately focus on a finite chain of cells and discretize the preceding partial differential equations. The discretization of this model forces us to consider an approximation to the spatial derivative operators in either Eq. (3.6) or Eq. (3.7). This choice leads to another layer of approximation on top of the approximation to the convolution operator.

For Eq. (3.6), the simplest approximation to $y''(z, t)$ is given by the centered finite-difference scheme,

$$y''(z, t) \approx \frac{y(z+a, t) - 2y(z, t) + y(z-a, t)}{a^2}, \quad (3.8)$$

where, again, $a = 1/m$ represents the size of each cell in the model. This discretization is a second-order approximation, meaning that the error induced is $O(a^2 y^{(3)})$. This choice coincides with the candidate convolution kernel

$$w^{(2,2)}(z) := \frac{1}{a^2}[\delta(z+a) - 2\delta(z) + \delta(z-a)], \quad (3.9)$$

where $\delta(z)$ represents the spatial Dirac delta. In this case, $\Gamma_1 = 1$ and the resulting model leads exactly to the NNLEGI model. The superscripts in $w^{(n,k)}$ denote that the kernel induces a k th-order discretization of the n th-order approximation to the convolution operator. Therefore, we have established a partial differential framework that encapsulates the NNLEGI model and provides a vehicle in which to understand the communication term through the theory of (linear) partial differential equations. It is this framework and connection that motivates us to consider additional communication mechanisms.

The choice of Eq. (3.9) effectively dictates that each cell can only communicate with its two adjacent cells per unit time. However, this modeling assumption need not hold, and we investigate in this paper the effect of assuming various ranges of cell communication per unit time. It is important to distinguish that in the following arguments we are not supposing that a cell can physically interact with nonadjacent cells, but simply that communication can reach a larger radius during a particular model time step. We will define the *radius*

of influence to be the number of cells directly engaged by the communication kernel in the communication process, per unit time. Obviously, the *radius of influence* for Eq. (3.9) is 3. With this in mind, we propose the alternative kernel

$$w^{(2,4)}(z) := \frac{1}{12a^2}[-\delta(z+2a) + 16\delta(z+a) - 30\delta(z) + 16\delta(z-a) - \delta(z-2a)], \quad (3.10)$$

which represents a fourth-order approximation to the second derivative term in Eq. (3.6), the induced error is $O(a^4 y^{(5)})$, and it effectively couples five cells per model time step, rather than 3.

While the kernel Eq. (3.10) provides a more accurate approximation to Eq. (3.6), we will want to consider kernels that also approximate Eq. (3.7). We can similarly discretize the fourth-degree spatial derivative using a simple central finite-difference scheme. A kernel that corresponds to a second-order approximation of the fourth-order spatial derivative is given by

$$w^{(4,2)}(z) := \frac{1}{a^4}[-\delta(z+2a) + 4\delta(z+a) - 6\delta(z) + 4\delta(z-a) - \delta(z-2a)], \quad (3.11)$$

for which $\Gamma_1 = 0$ and the second derivative term naturally drops out.

To summarize, there are two levels of approximation that we are exploring with these three candidate convolution kernels. When compared to a continuous convolution kernel, we have presented candidates that functionally act as a second- and fourth-order approximation to the convolution operator (3.2). These convolution approximations lead to partial differential equations with either second-order—Eq. (3.6)—or fourth-order—Eq. (3.7)—spatial derivatives in y . The discretization of these spatial derivatives leads to the second layer of approximation that must be made in the choice of finite-difference coefficients.

The candidate in Eq. (3.9) represents a choice that leads to the original NNLEGI model, which approximates both the convolution operator and subsequent spatial derivative operator with second-order approximations. The candidate $w^{(2,4)}$ in Eq. (3.10) also functions as an approximation to the continuous convolution operator with a second-order approximation, but it approximates the subsequent spatial derivative to fourth order. Importantly, this second candidate should behave similarly to $w^{(2,2)}$ in some respects, since both candidates approximate the same operator, but the latter candidate couples five cells in a given model time step. Finally, the candidate $w^{(4,2)}$ in Eq. (3.11) approximates the convolution operator to a higher order, i.e., fourth order, resulting in a higher spatial derivative that induces additional behaviors not captured by the preceding two candidates. Each of these approximations highlight important immediate physical characteristics that must be taken into account during the modeling process: the radius of influence and the characteristic of the derivative operator they are replacing. Our analysis will show that consideration of both the manner in which the convolution is approximated and the radius of influence play a role in the gradient sensing outcomes of the particular model.

Invoking these convolution kernel candidates leads to a discretization of Eq. (3.1) similar to Eq. (2.1) except with the generalization

$$\dot{y}_n = \beta r_n - \nu \sum_{n'=1}^m W_{nn'}^{(p,q)} y_{n'} + \chi_n.$$

The matrix $W_{nn'}^{(p,q)}$ has parameters p, q associated with the appropriate communication model $w^{(p,q)}$ described above (and appropriately chosen boundary conditions).

Before assessing how the various models of the communication mechanism impact gradient sensing, it must be emphasized that there is no *a priori* way of knowing which of these approximations is the one that captures the actual or appropriate biological communication mechanism. We will be using the term *approximation* to emphasize how a particular communication model is derived.

IV. ANALYSIS OF THE GENERAL AND APPROXIMATE MODELS

We now turn our attention to understanding how the competition between deactivation, communication, and thermal noise impacts the ability of the cells to perform gradient sensing via intercellular communication, as represented by the various alternative communication models. First, we analyze the mean dynamics in Fourier space with an aim of determining the rate at which disturbances travel through a network and whether the model acts as a filter. As such, it might amplify or suppress noise. We will also compare the various alternative communication models with regard to their gradient sensing capabilities, as measured by the SNR. Along the way, we will be interested in determining how the radius of influence impacts the outcomes.

A. Competition between deactivation and communication

We examine the role of deactivation and communication in the transient dynamics of y . The key parameters are ν and γ . The noise terms are additive in the rate equations, and we will drop these in order to focus on the mean dynamics. (Consideration of the noise will be taken up in the next subsection.) For some field $g(z, t)$, the Fourier transform is defined here as

$$\hat{g}(k, t) = \mathcal{F}(g) := \frac{1}{\sqrt{2\pi}} \int_{-\infty}^{\infty} g(z, t) e^{-ikz} dz. \quad (4.1)$$

Application of the transform to Eq. (3.1) yields

$$\begin{aligned} \dot{\hat{c}} &= -k^2 \hat{c} - \alpha \hat{c} + \mu \hat{r}, & \dot{\hat{y}} &= \alpha \hat{c} - \mu \hat{r}, \\ \dot{\hat{x}} &= \beta \hat{r} - \nu \hat{x}, & \dot{\hat{y}} &= \beta \hat{r} - \nu \hat{y} - \gamma \hat{w} \hat{y}, \end{aligned} \quad (4.2)$$

where $\hat{c}, \hat{r}, \hat{x}, \hat{y}, \hat{w}$ denote the Fourier counterparts to the original space variables. Note that $\hat{w}(k)$ is solely a function of the wave number k . The system of ordinary differential equations Eq. (4.2) is linear and can be represented by a system of equations whose eigenvalues are distinct for parameter values given in Table I. To explore model outcomes as a function of γ, ν , and the choice of model for communication, we consider the evolution of the system subject to a Dirac δ distribution for the initial concentration in y at $t = 0$. In this case, solving the

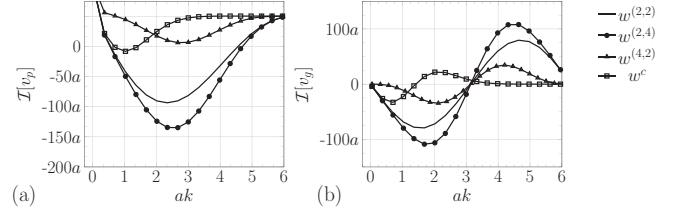


FIG. 1. (a) Phase velocities corresponding to three approximations, $w^{(2,2)}$, $w^{(2,4)}$, $w^{(4,2)}$, for the convolution term in Eq. (3.1), and for the Gaussian-inspired kernel w^n , plotted in units of a , the size of the cell. The nearest-neighbor model uses Eq. (3.9), while Eq. (3.10) uses a higher-order second derivative approximation, and finally Eq. (3.11) includes the fourth derivative term to the approximation, Eq. (3.7). (b) Similarly, the group velocities for these approximations, in units of a . Figures produced with parameters $\sqrt{\gamma/\nu} = 10$; smaller ratios decrease the magnitude of velocities, especially for $ak > 1$.

resulting differential equations gives

$$y(z, t) = \frac{1}{\sqrt{2\pi}} \int_{-\infty}^{\infty} \hat{y}(k, 0) e^{ikz} e^{-t[\gamma \hat{w}(k) + \nu]} dk. \quad (4.3)$$

From Eq. (4.3), it can be read off that the dispersion relation for this differential equation is given by

$$\omega(k) = i[\gamma \hat{w}(k) + \nu].$$

We note that $\gamma \geq 0$ and $\nu \geq 0$, with the physically relevant parameter regime $\gamma > \nu$. For this range of parameters, the solution is highly dispersive due to the communication mechanism. With the dispersion relationship in hand, the phase and group velocities are, respectively,

$$v_p = \omega(k)/k \quad \text{and} \quad v_g = \frac{d\omega}{dk}.$$

For $\sqrt{\gamma/\nu} = 10$, Figs. 1(a) and 1(b) depict the phase (v_p) and group velocities (v_g), respectively, for the various communication models and their associated $w^{(p,q)}$. We also include in this analysis the velocities for the continuous communication kernel Eq. (3.4). It is helpful to think of ak as an estimate of the roughness of the external gradient. We note that $\hat{w}(0) = 0$, since mass is conserved. For small wave numbers, $\hat{w}(k)/k \rightarrow 0$, while $\nu/k \rightarrow \infty$ (large wavelength) disturbances are primarily dominated by deactivation, with parameter ν , relative to communication with parameter γ . Large-scale disturbances are similar, regardless of the communication model.

It is in the analysis of the velocities at larger wave numbers where the physical interpretation of the convolution kernels and their impact on gradient sensing becomes significant. The qualitative analysis from these velocities will be critical to understanding the gradient precision calculations performed in Sec. IV B.

For larger wave numbers, the communication term dominates the dynamics. The communication term can potentially improve the discernment of signal structure by the cell network (as compared to a model with no communication term). The various alternative communication models handle small-scale disturbances differently, as is evident in the dispersion relations plotted in Fig. 1(a). The continuous case has the smallest dispersion and variation in the group velocity. Higher

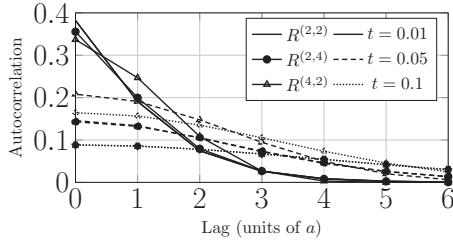


FIG. 2. Spatial autocorrelation $R^{(p,q)}(z, t)$ of Eq. (4.3) for the three communication kernels $w^{(2,2)}$, $w^{(2,4)}$, and $w^{(4,2)}$, respectively, plotted with lag in units of a . For each $R^{(p,q)}(z, t)$ the snapshots of the decaying autocorrelations are taken at times $t = 0.01$ (highest R at zero lag), 0.05 , and 0.1 (lowest R at zero lag). Autocorrelations of the two second derivative approximations, $w^{(2,2)}$ and $w^{(2,4)}$, are nearly indistinguishable for $t \geq 0.05$. Here $\sqrt{\gamma/\nu} = 10$.

dispersion, as is evident in the alternative models, means that a signal will develop a time and space dependence as it propagates through the network. In the large wave-number regime, the phase velocity is monotonic for the model associated with w^n , but not for the other (truncated) approximations. We see from Fig. 1 that the various models induce differences in qualitative and quantitative behavior.

Analyzing the candidate kernels in Fig. 1, both $w^{(2,2)}$ and $w^{(2,4)}$ induce velocities that are similar quantitatively and qualitatively, and these in turn are different from $w^{(4,2)}$ quantitatively. In particular, there is a slight shift in the peaks of the velocities of $w^{(4,2)}$ toward larger wave numbers. The figures suggest that the choice of communications model is more critical than the radius of influence in modeling gradient sensing differences. The continuous kernel, too, has a shift in the peak, but toward smaller wave numbers. For wave numbers greater than the cell size, we expect interaction with noisier parts of the signal spectrum. Therefore, both the scale and location of the peaks of these velocities impact the amplification of noise. Since the continuous kernel has phase velocity peaks of much lower relative magnitude that also center around smaller wave numbers, we expect this kernel to induce better cellular precision and a higher signal-to-noise ratio when compared to the discrete convolution kernels—but the precise extent of this impact is indeterminable from Fig. 1. The impact of the placement and scale of the peaks of the velocities corresponding to $w^{(4,2)}$, in particular, would possibly indicate both higher precision—because the magnitude of velocities corresponding to larger wave numbers is small—but also lower precision—because the peak of the velocities is skewed toward much noisier frequencies.

In summary of our dispersion analysis, the dispersion relation suggests that the competition between deactivation and communication leads to a nontrivial transient aspect to gradient sensing and transport and thus to a coupling of space and time (with a finite correlation length) of the signaling process.

We also consider the autocorrelation of the solution Eq. (4.4) induced by the three discrete convolution kernels. Autocorrelation, a measure of the spatiotemporal coupling that results in the competition of the deactivation and communication, is quantified in Fig. 2 and denoted by $R^{(p,q)}$ for the various models $w^{(p,q)}$. $R^{(2,2)}$ and $R^{(2,4)}$ are comparable in

space and time and nearly identical for $t \geq 0.05$, while $R^{(4,2)}$ has a noticeably longer sustained autocorrelation. It appears again that the radius of influence has a smaller impact on physical results when compared to the nature of the model: it is the analytic properties of $w^{(4,2)}$ and the nature of its approximation to the convolution term that induce a much larger lag for a given time and therefore a more complicated communication model.

Finally, a simple calculation following Eq. (4.3) provides a deeper layer of insight into this competition between communication, diffusion, and deactivation in the transient phase. The analysis will focus on the second-order model truncation, which can be carried farther analytically, but it is clear from what follows that the fourth-order differential operator approximation would yield a similar procedure and story. Assuming $\hat{w}(k)$ is sufficiently smooth, we can represent it in terms of a Taylor expansion about a cell location, which we truncate at the quadratic term. Keeping our original assumptions about w (w is even), we can simplify this series and write the stationary-phase solution as

$$y(z, t) \approx \frac{e^{-t\nu}}{2\pi} \int e^{-i[kz - i\gamma k^2/2\hat{w}''(0)t]} dk, \quad (4.4)$$

for which a closed-form solution for an approximation of $y(z, t)$ exists, viz.,

$$y(z, t) \approx \frac{e^{-t\nu - \frac{z^2}{2\hat{w}''(0)\gamma t}}}{\sqrt{2\pi \hat{w}''(0)\gamma t}}, \quad (4.5)$$

where $\hat{w}''(0)$ is understood to be the coefficient of the second-order term in \hat{w} . Having this expression enables a fruitful analysis of the species' dependence on the parameters ν , γ .

There are three immediate conclusions that can be drawn from formula (4.5). First, for a fixed t , γ affects the variance of the distribution of y . This matches the intuition and physical reasoning that γ , being the communication parameter, diffuses the species y among the cells in the system. Similarly, ν acts only as a rate of exponential decay. This again intuitively matches our expectation that ν controls the rate of deactivation of y . Lastly, when t is relatively small, the importance of the diffusive term, and thus γ and the choice of communication model, are greater than ν . Setting the argument of the exponential in Eq. (4.5) to zero, it is possible to find a space/time horizon, which is approximately defined as $z/t = \pm\sqrt{\nu 2\hat{w}''(0)\gamma}$. Taking this into account and the decaying nature of y as a function of time, it is thus expected that the autocorrelation of y begins compact, decays to zero for large distances, and relaxes in time. With this analysis, it is not difficult to reason about the behavior of more general kernels than those considered here, especially those that do not respect spatial symmetry, which would manifest in advective-like behaviors.

B. Signal-to-noise ratio

Having focused on the competition of deactivation and communication, we now consider how these forces are affected by the presence of noise intrinsic and extrinsic to each cell in the network. In [14] it is argued that gradient sensing for a given network can be assessed by computing the SNR

of the difference between the internal and communication signals relative to the noise in the system (see below for the precise definition). In this section, we derive the SNR again and analyze the SNR induced by the four convolution kernel candidates considered heretofore.

In the first step in our SNR derivation, we give the mean steady-state solutions to Eq. (3.1). Assuming appropriate boundary conditions, we denote \bar{c} as the steady-state solution for the concentration c , which satisfies $\nabla^2 c = 0$. A simple form for the concentration c that obeys this equation and boundary conditions varies linearly in space with slope g such that $ag/\bar{c} \ll 1$. We will assume this form for \bar{c} . The remaining steady-state solutions are

$$\begin{aligned} \bar{r} &= \frac{\alpha}{\mu} \bar{c}, & \bar{x} &= \frac{\beta}{\nu} \bar{r} = \frac{\beta\alpha}{\mu\nu} \bar{c}, \\ \bar{y} &= \mathcal{F}^{-1} \left\{ \frac{\frac{\beta}{\nu} \mathcal{F}(\bar{r})}{1 + \frac{\gamma}{\nu} \mathcal{F}(w)} \right\} = \frac{\alpha\beta}{\mu\nu} \mathcal{F}^{-1} \left\{ \frac{\mathcal{F}(\bar{c})}{1 + \frac{\gamma}{\nu} \mathcal{F}(w)} \right\}, \end{aligned} \quad (4.6)$$

where \mathcal{F} is the spatial Fourier transform defined previously. Now, turning to the discrete setting for the rest of this section, the last line in Eq. (4.6) becomes

$$\bar{y}_n = \frac{\alpha\beta}{\mu\nu} \sum_{n'=1}^m K_{nn'}^{(p,q)} \bar{c}_{n'}, \quad (4.7)$$

where $K_{nn'}^{p,q} = (W^{p,q})_{nn'}^{-1}$. When $\gamma = 0$, there is no communication, and $\bar{y} = \bar{x}$. When the communication term is nonzero, the deviation of \bar{y} from \bar{x} provides an indication of the impact of communication on the system and if the cell is near higher concentrations of c . To this end, we follow [14] and define the following deviation of mean states:

$$\bar{\Delta}_n = (\bar{x}_n - \bar{y}_n). \quad (4.8)$$

The ability for a cell to detect the gradient of the external chemical field among a noisy background is the ratio of the square of this mean deviation and the variance in species concentrations of x , y ,

$$\text{SNR} = \left(\frac{\bar{\Delta}_n}{\delta\Delta_n} \right)^2, \quad (4.9)$$

where $(\delta\Delta_n)^2 = (\delta x_n)^2 + (\delta y_n)^2 - 2C_{nn'}^{xy}$, and $C_{nn'}^{xy}$ is the cross-correlation between x and y . To calculate the variances, we start by computing the power spectra of r , x , and y : S^{rr} , S^{xx} , and S^{yy} . We must make a series of assumptions for the relevant timescales: the integration time T is longer than the receptor equilibration time, messenger turnover time ($1/\nu$), and messenger exchange time ($1/\gamma$) (we borrow these assumptions from [14], which describes them in more detail). Under these assumptions, covariances in long-time averages are given by the low-frequency limits of the power spectra, $C_{nn'}^{xy} = \lim_{\omega \rightarrow 0} S_{nn'}^{xy}(\omega)$. In the discrete setting, Ref. [14] invokes the fluctuation-dissipation theorem, makes a linear noise approximation, and provides a derivation of S_n^{rr} , which we use unaltered in our generalization,

$$S_{nn'}^{rr}(\omega) = \frac{2\alpha\bar{c}_n}{\mu^2} \begin{cases} 1 + \frac{\alpha}{2\pi aD}, & n' = n, \\ \frac{\alpha}{4\pi aD} \frac{1}{|n-n'|}, & n' \neq n. \end{cases} \quad (4.10)$$

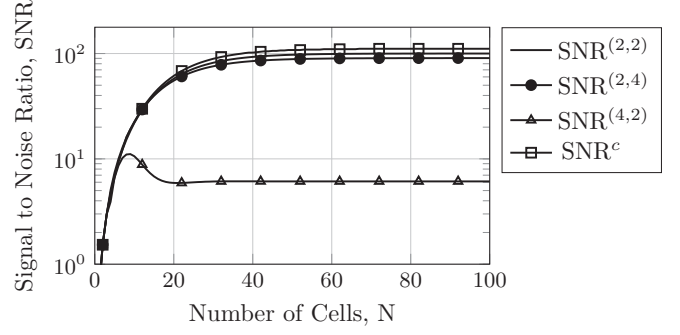


FIG. 3. Precision of gradient sensing with temporal integration. Signal-to-noise ratio $\text{SNR}^{(p,q)}$, defined as Eq. (4.9), when using approximations $w^{(2,2)}$, $w^{(2,4)}$, and $w^{(4,2)}$. $\text{SNR}^{(4,2)}$. Here, N refers to the number of cells in the system. We use $\alpha/a^3\mu = \beta/\nu = 100$, $D = 50 \mu\text{m}^2/\text{s}$, $a = 10 \mu\text{m}$, $\mu = \nu = 1 \text{ s}^{-1}$, $T = 10 \text{ s}$, and $\sqrt{\gamma/\nu} = 10$. Parameter values as suggested in [14].

The power spectra $S_{nn'}^{xx}$, $S_{nn'}^{yy}$, and $S_{nn'}^{xy}$ can more easily be computed by calculating the (co)variances of the Fourier transforms of Eq. (3.1) in space and time,

$$\begin{aligned} S_{nn'}^{xx}(\omega) &= \langle \mathcal{F}(\delta x_n)^* \mathcal{F}(\delta x_{n'}) \rangle \\ &= \frac{1}{\nu^2 + \omega^2} [S_{nn'}^{rr}(\omega) + \langle \mathcal{F}(d\xi_n)^* \mathcal{F}(d\xi_{n'}) \rangle], \end{aligned} \quad (4.11)$$

$$\begin{aligned} S_{nn'}^{yy}(\omega) &= \langle \mathcal{F}(\delta y_n)^* \mathcal{F}(\delta y_{n'}) \rangle \\ &= \frac{1}{\nu^2} \sum_{jj'} \tilde{K}_{nj}^{p*} \tilde{K}_{n'j'}^p [S_{jj'}^{rr}(\omega) + \langle \mathcal{F}(d\chi_j)^* \mathcal{F}(d\chi_{j'}) \rangle], \end{aligned} \quad (4.12)$$

and

$$S_{nn'}^{xy}(\omega) = \langle \mathcal{F}(\delta x_n)^* \mathcal{F}(\delta y_{n'}) \rangle = \frac{1}{\nu(\nu + i\omega)} \sum_j \tilde{K}_{nj}^p S_{nj}^{rr}(\omega), \quad (4.13)$$

where $\tilde{W}_{nn'} := W_{nn'} - i(\nu/\omega)\delta_{nn'}$. The spectra of the thermal noise terms $d\xi_n$ and $d\chi_n$ can be calculated using the steady-state means and Fourier transform in a similar way to get, respectively,

$$\begin{aligned} \langle \mathcal{F}(d\xi_n)^* \mathcal{F}(d\xi_{n'}) \rangle &= 2\nu\bar{x}_n, \\ \langle \mathcal{F}(d\chi_n)^* \mathcal{F}(d\chi_{n'}) \rangle &= 2\nu W_{nn'}^{(p,q)}. \end{aligned} \quad (4.14)$$

Finally, combining Eq. (4.11) into the definition of $(\delta\Delta_n)^2 = (\delta x_n)^2 + (\delta y_n)^2 - 2C_{nn'}^{xy}$ and Eq. (4.9) allows us to compute a metric for the ability of the cells to extract gradient information from a noisy background. In Fig. 3, we depict the SNR corresponding to the various approximations to $w^{(p,q)}$: Eqs. (3.9), (3.10), and (3.11) yield the curves $\text{SNR}^{(2,2)}$, $\text{SNR}^{(2,4)}$, and $\text{SNR}^{(4,2)}$, respectively, as a function of system size.

For large cell numbers, the precision of gradient sensing when including more accurate approximations to the

convolution seemingly degrades. This provides a clue to our analysis from Fig. 1 that the location of the peak of the phase velocities has a larger impact on the signal-to-noise ratio than the peak's magnitude. We also see that the Gaussian-inspired kernel induces the greatest sensory precision of the models tested. The radius of influence does not appear to be the critical aspect, since the SNR of $w^{(2,4)}$ is similar to the nearest neighbor's SNR; rather, the analytic properties associated with each parametrization are more aligned with model outcomes. We find that the use of the fourth derivative approximation $w^{(4,2)}$ has a dramatic impact on the ability of cells to determine the gradient of the external chemical field. For large system size, and a high-order approximation of the kernel, the gradient sensing degrades by an order of magnitude. The impact of the more effective communication model (see Fig. 2) is to propagate more information from noisy frequencies.

V. SUMMARY AND CONCLUSIONS

Gradient sensing in chains of cells and organisms that have no specialized gradient sensing organelles is not well understood. Experimental evidence lends support to the conjecture that the ability of chains of cells to sense the gradient of an external chemical species' concentration could involve cell-to-cell communication. This hypothesis is central to a local excitation global inhibition (LEGI) model proposed by Mugler *et al.* [14] (we denoted it here as the NNLEGI model). In this particular LEGI model, communication is restricted to nearest-neighbor communication. Using physically inspired parameters and a measure of signal discernment between internal and neighboring inputs, relative to the background noise, they showed that their modeled cell chain could sense this external gradient.

Given that there is no *a priori* reason to assume that cell communication, in a single model time step, is only effected with nearest neighbors, a significant consideration for pursuing gradient sensing via communication is the range of communicating cells, as it directly impacts the cell concentration, SNR, and thus the overall capability of the cell to sense a gradient. In contrast to diffusive processes, the communication process modeled via a convolution has a finite speed of signal communication, and thus it makes sense to analyze generally how disturbances are affected by a competition of dissipation and competition, all the while taking into account local background noise.

In this paper, we replaced the nearest-neighbor communication term in the NNLEGI model by a more general convolution-dependent model. By generalizing, we aimed to explore how the gradient sensing capabilities of the model depend on the radius of influence as well as on the approximating order of the convolution kernel itself. The radius of influence refers to the number of neighbors involved in the communication, per unit time. The approximating order refers in turn to how the convolution kernel is approximated locally. The NNLEGI model was shown to be subsumed into the more general model, and thus we also furthered the analysis of the original nearest-neighbor model as well.

The generalized model was analyzed with the aim of establishing how cell size, cell chain length, and alternative proposals for the intercellular communication mechanisms manifest themselves in the gradient sensing model outcomes.

Our analysis of the general model shows that the manner in which information was shared and the properties of the convolution approximation are more critical to the precision of gradient sensing than the radius of influence alone. We found that the choice of communication parametrization (model) produced meaningful differences on model outcomes like information velocities (Fig. 1), signal autocorrelation (Fig. 2), and the SNR (Fig. 3). Further, we determined spatiotemporal ranges where one expects to see deactivation-dominated or advective-dominated (via communication) reactions and how the sensitivity of the model was related to those parameters and the choice of the communication kernel.

We found that the NNLEGI exhibits high SNR as compared to a model equipped with higher-order approximations for the communication. The NNLEGI and the continuous Gaussian-inspired kernel mode for communication had comparable SNR. However, the discrete nature of the various approximations, *vis-à-vis* the continuous kernel convolution, lead to dispersive signaling, affecting both the coherence of the signal as well as propagation of background noise. The dispersion relation of the models with second order, and the fourth-order approximations to the second-order spatial derivative, were similar to each other but were not similar to the continuous Gaussian-inspired kernel. The model that approximates the convolution to the fourth order, however, exhibits a significantly lower SNR as a consequence of more effective communication and propagation of higher-frequency information. As a result, it is more prone to propagate frequencies corresponding to thermal noise.

The introduction of a communication aspect to gradient sensing in models for chains of cells introduces nuances related to finite-time signal propagation that need to be considered in making comparisons with the physical systems they model. Both the discernment of signals in a noisy environment and transient behavior should be a consideration in developing a LEGI model for gradient sensing that compares well with observations. Understanding how communication models impact gradient sensing, it is argued here, could lead to better models for gradient sensing, but more importantly, to a better basic understanding of how cells and collections of these sense an external gradient.

ACKNOWLEDGMENTS

We thank A. Mugler and B. Sun for fruitful discussions. J.M.R. wishes to thank the Kavli Institute of Theoretical Physics (KITP) at the University of California, Santa Barbara, for their hospitality and for supporting his research on this project. The KITP is supported in part by the National Science Foundation under Grant No. NSF PHY-1748958. C.V. and B.F. were Research Experiences for Undergraduate participants at Oregon State University in summer of 2017. The REU program is sponsored by the National Science Foundation under Grant No. NSF DMS-1359173. The submitted manuscript has been authored by a contractor of the U.S. Government under Contract No. DE-AC05-00OR22725. Accordingly, the U.S. Government retains a non-exclusive, royalty-free license to publish or reproduce the published form of this contribution, or allow others to do so, for U.S. Government purposes.

- [1] H. Berg and E. Purcell, Physics of chemoreception, *Biophys. J.* **20**, 193 (1977).
- [2] C. A. Parent and P. N. Devreotes, A cell's sense of direction, *Science (NY)* **284**, 765 (1999).
- [3] A. Levchenko and P. A. Iglesias, Models of eukaryotic gradient sensing: Application to chemotaxis of amoebae and neutrophils, *Biophys. J.* **82**, 50 (2002).
- [4] B. A. Camley, J. Zimmermann, H. Levine, and W.-J. Rappel, Collective signal processing in cluster chemotaxis: Roles of adaptation, amplification, and co-attraction in collective guidance, *PLoS Comput. Biol.* **12**, e1005008 (2016).
- [5] D. Ellison, A. Mugler, M. D. Brennan, S. H. Lee, R. J. Huebner, E. R. Shamir, L. A. Woo, J. Kim, P. Amar, I. Nemenman, A. J. Ewald, and A. Levchenko, Cell-cell communication enhances the capacity of cell ensembles to sense shallow gradients during morphogenesis, *Proc. Natl. Acad. Sci. (USA)* **113**, E679 (2016).
- [6] E. F. Keller and L. A. Segel, Initiation of slime mold aggregation viewed as an instability, *J. Theor. Biol.* **26**, 399 (1970).
- [7] P. Friedl and D. Gilmour, Collective cell migration in morphogenesis, regeneration and cancer, *Nat. Rev. Mol. Cell Biol.* **10**, 445 (2009).
- [8] E. Theveneau, L. Marchant, S. Kuriyama, M. Gull, B. Moepps, M. Parsons, and R. Mayor, Collective chemotaxis requires contact-dependent cell polarity, *Develop. Cell* **19**, 39 (2010).
- [9] R. G. Endres and N. S. Wingreen, Accuracy of direct gradient sensing by cell-surface receptors, *Prog. Biophys. Mol. Biol.* **100**, 33 (2009).
- [10] B. Hu, W. Chen, W.-J. Rappel, and H. Levine, Physical Limits on Cellular Sensing of Spatial Gradients, *Phys. Rev. Lett.* **105**, 048104 (2010).
- [11] A. Jilkine and L. Edelstein-Keshet, A comparison of mathematical models for polarization of single eukaryotic cells in response to guided cues, *PLoS Comput. Biol.* **7**, e1001121 (2011).
- [12] B. Hu, W. Chen, H. Levine, and W.-J. Rappel, Quantifying information transmission in eukaryotic gradient sensing and chemotactic response, *J. Stat. Phys.* **142**, 1167 (2011).
- [13] G. Malet-Engra, W. Yu, A. Oldani, J. Rey-Barroso, N. S. Gov, G. Scita, and L. Dupré, Collective cell motility promotes chemotactic prowess and resistance to chemorepulsion, *Curr. Biol.* **25**, 242 (2015).
- [14] A. Mugler, A. Levchenko, and I. Nemenman, Limits to the precision of gradient sensing with spatial communication and temporal integration, *Proc. Natl. Acad. Sci. (USA)* **113**, E689 (2016).
- [15] R. J. Leveque, Finite difference approximations, in *Finite Difference Methods for Ordinary and Partial Differential Equations* (SIAM, Philadelphia, 2007), Chap. 1, pp. 3–11, <https://epubs.siam.org/doi/pdf/10.1137/1.9780898717839.ch1>.
- [16] J. D. Murray, *Mathematical Biology* (Springer, New York, 2002).

Correction: The omission of a support statement in the Acknowledgment section has been fixed.